Low-Illumination Image Enhancement Algorithm Based on a Physical Lighting Model

Shun-Yuan Yu and Hong Zhu

***Abstract*— Low-illumination images are usually taken in non-uniform environmental light, such as extremely dark or bright light or artificial light. The enhancement results achieved by existing techniques are prone to halo artifacts, color unnaturalness, and information loss. To address these problems, we present a physical lighting model that describes the degradation of poor illumination images, in which the environmental light is a point-wise variable and changes with the local light source. As long as the parameters in the model are properly estimated, the low-illumination images can be directly recovered by solving the model. First, the initial environmental light can be considered as the incident component according to the Retinex theory and estimated via a Gaussian surrounding function. Second, the environmental light and light-scattering attenuation rate are iteratively adjusted with the information loss constraint. Finally, to restrain the halo and block effects, the two parameters are refined by the weighted guide filter. The experimental results indicate that the proposed algorithm can improve the appearance of low-illumination images that are captured in different scenes, reveal the details in textured regions with few halo effects, increase the richness of the visible edges, retain color consistency and reproduce the color quality and naturalness.**

***Index Terms*— Image enhancement, low-illumination image, physical lighting model, contrast enhancement, weighted guide filter.**

I. Introduction

IMAGES that are captured in low-illumination conditions such as night vision, shadow or backlit conditions, usually exhibit low global contrast and small grayscale distribution, which cause content blur and detail loss in dark regions. In addition, artificial light can cause uneven global brightness and overexposure or underexposure in some regions, which may hinder identification of the information in regions of interest and limit the performance of outdoor vision systems. Therefore, low-illumination images should be recovered by enhancing the detail in dark regions, restraining the overexposure regions, and improving the global contrast and dynamic range.

Manuscript received July 20, 2016; revised February 21, 2017, July 2, 2017, and September 12, 2017; accepted October 1, 2017. Date of publication October 16, 2017; date of current version January 7, 2019. This work was supported in part by the National Natural Science Foundation of China under Grant 61673318 and in part by the High-Level Talent Project of Ankang University under Grant 2017AYQDZR01. This paper was recommended by Associate Editor K. Ma. *(Corresponding author: Hong Zhu.)*

S.-Y. Yu is with the Faculty of Automation and Information Engineering, Xi'an University of Technology, Xi'an 710048, China, on leave from the Faculty of Electronics and Information Engineering, Ankang University, Ankang 725000, China (e-mail: ysywzhm@163.com).

H. Zhu is with the Faculty of Automation and Information Engineering, Xi'an University of Technology, Xi'an 710048, China (e-mail: zhuhong@xaut.edu.cn).

Color versions of one or more of the figures in this paper are available online at http://ieeexplore.ieee.org.

Digital Object Identifier 10.1109/TCSVT.2017.2763180

Various algorithms have been developed to address the aforementioned problems; one of the most extensively utilized and simplest approaches is the histogram equalization (HE) [1]. The objective of HE is to redistribute the grayscale probability across the entire dynamic range, which enhances the global contrast; however, the uniform redistribution of the histogram merges some of the grayscales, which induces noise in the dark regions. This approach does not consider local content, creates artifacts in smooth regions and degrades sharpness at the boundaries. Thus, several improved methods [2]–[5] that are based on HE have been proposed to overcome these shortcomings. For example, Singh and Kapoor [4] recently presented an Exposure-based Sub-Image Histogram Equalization (ESIHE) method to enhance low-exposure images. ESIHE can improve the contrast; however, the enhancement rate is controlled by the exposure thresholds, which causes brightness diffusion in bright regions. Considering human visual attention, Jung and Sun [6] combine HE method with tone mapping for contrast enhancement, which can restrain over enhancement in smooth regions, but may restore limited sharpness at the edges.

Another category of complex methods are those based on Retinex [7] and multi-scale Retinex (MSR) [8] algorithm. To improve the efficiency of the MSR algorithm for real-time applications, Jiang *et al.* [9] presented a parallel algorithm that employs a graphics processing unit (GPU). To compensate for color under-saturation due to MSR algorithm, Petro *et al.* [10] offered a color correction final step. The MSR algorithm and its extension methods have high computational complexity. Halo effects around the regions in which light rapidly changes and the performance for low-illumination images is limited in extremely dark and overexposed regions.

Filter-based methods are primarily aimed at filtering noise and improving the dynamic range by applying tone or histogram adjustments. Lee *et al.* [11] removed the noise in low-light level images using a noise-adaptive spatial-temporal filter, which can improve the signal-to-noise ratio, but attained limited performance improvements in very dark images. Xu *et al.* [12] adapted the Non-Local Means method for denoising, and enlarged the dynamic range by performing tone adjustment, which achieves significant noise removal; nevertheless, the restored sharp edges and details appear blurred. Minjae *et al.* [13] utilized Kalman filter to remove noise in low-light-level images, and broadened the contrast and dynamic range by applying Gamma correction and histogram clipping. Schettini *et al.* [14] presented a local image content exponential correction technique that is based on a bilateral filter, which can simultaneously present overexposed

and underexposed regions well; however, the restored color lacks vividness.

The previously mentioned methods improve low-illumination images according to the image enhancement concept, but do not consider physical lighting of low-illumination images. Thus, the enhanced results lack local details in rich texture regions and vividness in color renditions. Consequently, physical model based methods have been developed in recent years. Dong *et al.* [15] and Zhang *et al.* [16] assumed that the inverted input low-illumination images are similar to images that are acquired in the presence of substantial haze, and the haze model and dark channel prior (DCP) [17] are applied to restore low-illumination images. However, DCP is effective for daytime outdoor images, but cannot adapt to the low-illumination images. Cao *et al.* [18] derived the brightness baseline model and enhanced the low-illumination traffic images with color image compensation. Dong and Wen [19] proposed the local maximum color value (LMCV) prior; combined with the haze image degradation model [20], they recovered the low-illumination images. However, the degradation model for the haze images cannot adequately reflect the globally changing illumination, and the detail in the very dark regions of the restored image is limited. This method requires additional exposure adjustment, and the LMCV prior does not apply to the artificial light scenes and the restored results lack naturalness. Zhang *et al.* [21] presented a new nighttime hazy imaging model that accounts for both the non-uniform illumination from artificial light sources and the scattering and attenuation effects of the haze. This method, which is referred to as NHRIC, can achieve illumination balance for low-illumination images but induces heavy pseudo color in dark regions; the enhancement is not content-aware and lacks naturalness. To preserve naturalness while enhancing the details in non-uniform illumination images, Wang *et al.* [22] proposed a bi-log transformation to map the illumination to create a balance between the details and the naturalness, this is referred to as the naturalness-preserving enhancement algorithm (NPEA).

The majority of these model-based methods are directly based on the haze degradation model with constant atmospheric light. But for low-illumination images, environmental light primarily consist of artificial light, i.e., it changes with the local content. Thus, images captured with low-illumination are degraded with the scene depth and the corresponding environmental lights; the signal-to-noise ratio is low, and the information loss during the enhancement should be limited. To overcome these problems, we analyze the physical imaging process of low-illumination images, set up the degradation model, and adaptively enhance the low-illumination images according to the model and local image content with the information loss constraint.

Compared with other existing methods, the main contributions of our algorithm are as follows:

1) To account for the non-uniform environmental light, a new physical lighting model is presented for low-illumination images. The model has two main parameters: the environmental light and the light-scattering attenuation rate. The parameters are point-wise variables and change with the local content of the images. According to the Retinex theory, the initial environmental light is considered as the incident component of the low-illumination image, and estimated through a Gaussian filter.
2) The information loss is considered during the process of illumination correction. Using the useful information loss constraint, the environmental light and light-scattering attenuation rate in the model are estimated through iterative adjustment. Thus, it elegantly bypasses the most commonly employed HE and MSR methods. The restored results can effectively reveal the local details and can avoid over-enhancement with limited information loss.
3) To alleviate the halo and block artifacts, we refine the coarse environmental light and light-scattering attenuation rate using a weighted guide filter [23]. Because color consistency is another important factor between the restored results and the input image, we only enhance the intensity channel of the input image in HSV color space. Thus, we can restore the low-illumination image with less color distortion; the restored color is vivid, colorful and natural.

The remainder of the paper is organized as follows: in Section II we analyze the physical imaging process of low-illumination images and set up the degradation model. Section III presents a detailed description of the parameters estimation in the model, and the model's applicability for low-illumination image restoration. Section IV presents and compares the experimental results produced by seven methods for images that representing different scenes, including qualitative and quantitative assessment. Our conclusions are presented in Section V.

II. Physical Lighting Model

In this section, we propose a novel physical lighting model to depict images that are captured during low-illumination conditions, such as nighttime, sunrise, sunset and so on.

As concluded by McCartney [24], the light that reaches to the camera is composed of direct transmission light and atmospheric scattering light. The direct transmission light is part of the object reflection light, which is not scattered by the atmospheric particles; it comprises the remaining part of the energy attenuation. The atmospheric scattering light is part of the scattered environmental light that reaches a camera. The environmental light usually comprises direct sunlight, the diffusion of sky brightness, the reflection of the ground, the emitting of night source light and so on.

The degradation model [20] that consists of direct attenuation term and scattering light term, is inferred from McCartney's scattering theory and has been widely employed in haze removal methods [17], [25]–[27]. The premises of the model are that the existence of atmospheric particles, and environmental light should be constant. In the case of low-illumination images, there are similarities as well as differences with hazy images. First, the scattering particles are everywhere, even on sunny clear days [17],

the scattering phenomenon caused by which is a cue of the aerial perspective [28]. Thus, the existence of light scattering is necessary in low-illumination images, and the model to depict the degradation of low-illumination images should also consist of the two terms: direct attenuation term and scattering light term; however, as analyzed before, the environmental light in low-illumination image primarily consists of artificial light, which is neither homogenous nor constant. It is difficult to give an explicit expression which depicts the changes of the incident light at different scene points. As a result, they are assumed to be local variables in this paper.

Based on the above analysis, we propose a physical lighting model to depict the degradation of low-illumination images. Mathematically, it can be expressed as follows:

$$S(x, y) = R(x, y) \cdot t(x, y) + L(x, y) \cdot (1 - t(x, y)), \quad (1)$$

where $S(x, y)$ is the observed low-illumination image, $R(x, y)$ is the target image that to be restored; $t(x, y)$ is the light-scattering attenuation rate with the range of $[0, 1]$, which accounts for the ratio of light that is not scattered and reaches the camera; $L(x, y)$ is the environmental light, different from the constant environmental light in the typical hazy model, it is a point-wise variable and changes with the local scene light source.

When $t(x, y)$ and $L(x, y)$ are reliably estimated, the target image $R(x, y)$ can be achieved by solving model (1), as shown in (2):

$$R(x, y) = (S(x, y) - L(x, y))/\max(t_{\min}, t(x, y)) + L(x, y), \quad (2)$$

where, $t_{\min}$ is the lower bound of $t(x, y)$, which is set to avoid the overflow. We experimentally set $t_{\min}$ to 0.1, because an excessively small value of $t_{\min}$ would render the restored image prone to noise as discussed in [17].

III. Proposed Method

Given an input low-illumination image, solving the variables in Eq. (1) is indeed an ill-posed problem; it seems more difficult for the point-wise variable $L(x, y)$ in the proposed new model. In this section, we proposed an algorithm to restore the low-illumination images, which relies on the physical lighting model and information loss constraint. We assume that a restored image should have as high contrast as possible, and thus find the optimal light-scattering attenuation rate $t(x, y)$ value for each local watching window through a iterative adjustment with the constraint of information loss.

The proposed low-illumination image enhancement algorithm mainly consists of four sequential steps as shown in Fig. 1, i.e., the initial environmental light estimation, environmental light compensation and light-scattering attenuation rate estimation, refinement for parameters and low-illumination image restoration. First of all, the initial environmental light is estimated on the basis of Retinex theory. Next, Eq. (1) is solved with the estimated initial environmental light and the given initial light-scattering attenuation rate for each local watching window. Then, the information loss is calculated for each local watching window. If the maximum iteration times are not reached and the information loss is larger than the preset threshold, the environmental light and the light-scattering attenuation rate are adjusted as well. Otherwise, the iteration will be stopped, followed, the environmental light and light scattering attenuation rate are refined through a weighted guide filter. Finally, the low-illumination images can be recovered using the achieved parameters.

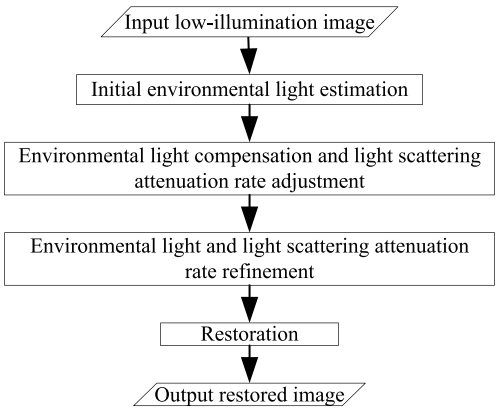

Fig. 1. Block diagram of the proposed low-illumination image enhancement algorithm.

A. Initial Environmental Light Estimation

Environmental light in low-illumination image primarily consists of artificial light, which is neither homogenous nor constant. It is difficult to give an explicit expression to depict the changes of the incident light at different scene points. In our algorithm, once the initial environmental light is estimated, the final environmental light can be achieved through iterative adjustment with the information loss constraint.

The initial environmental light can be considered as the incident component of an image. Thus, we can estimate the initial environmental light for low-illumination images according to the Retinex theory. As evaluated by Jobson *et al.* [29] that a Gaussian form surround function observes a better performance in extracting the incident component. Therefore, in our algorithm, we estimate the initial environmental light through a Gaussian filter, can be expressed as follows:

$$L_{ini}(x, y) = S(x, y) * F(x, y), \quad (3)$$

where $L_{ini}(x, y)$ is the initial environment light, "$*$" denotes the convolution operation, and $F(x, y)$ is the Gaussian shape surround function, as shown in (4):

$$F(x, y) = \lambda e^{\frac{-(x^2+y^2)}{c^2}}, \quad (4)$$

where, c reflects the standard deviation σ of the Gaussian filter and it is further related to the Gaussian convolution window size d, controls the amount of spatial detail which is retained; λ is a normalized factor that:

$$\iint F(x, y)dxdy = 1, \quad (5)$$

As indicated by Jobson *et al.* [29] and Petro *et al.* [10], the value of σ cannot be theoretically modeled and determined.

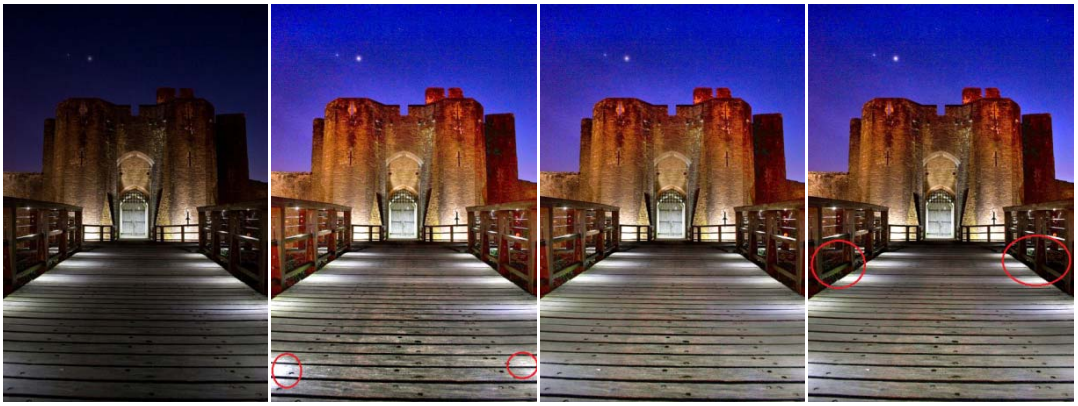

Fig. 2. Restoration effects with different local watching window sizes. An original low-illumination image is show in (a); the corresponding restored images via different local window sizes are reported in (b)-(d).

As far as our algorithm concerned, with the scattering chrematistics of light source, we assume that the illumination is local smooth, so it shouldn't retain too many details. Thus, σ cannot be too small, however, if the light source is in the distance, σ cannot be too large. According to a series of experiments, we set $\sigma = 10$ pixels and the Gaussian convolution window size $d = 20$ pixels as a reasonable compromise.

B. Initial Environmental Light Compensation and Light Scattering Attenuation Rate Estimation

The initial environmental light extracted from the original low-illumination can be very dim in underexposed regions or too bright in overexposed regions, which should be properly compensated to correct the brightness for poorly lit images. The light-scattering attenuation rate in our algorithm is defined as the ratio of light that is not scattered and reach to the camera, ranging from 0 to 1. In this paper, the environmental light compensation and the light-scattering attenuation rate estimation are both achieved with the information loss constraint based on the model (1).

As to a 8-bit bitmap file, the information loss occurs when the computed pixel values are outside the valid display dynamic range [0, 255], and the underflow part and overflow part will be truncated to 0 and 255, respectively. Consequently, the scene information of the corresponding regions is lost, and visually, appears like a "black hole" or "overexposure", which is the so called information loss. Kim *et al.* [30] inferred that the contrast of a hazy image is proportional to the information loss, whereas the restored contrast is inversely proportional to transmission. We found the same relationship among the light-scattering attenuation rate, contrast and information loss in low-illumination images. Therefore, to maximize the contrast of low-illumination images, the light-scattering attenuation rate should be as low as possible; however, the information loss should meet the pre-set threshold N_{th} at the same time. With this theory, we estimated the light-scattering attenuation rate and compensated the environmental light via iterative adjustment with the information loss constraint.

We assume that the illumination and depth are local smooth, and find a constant light-scattering attenuation rate value for each local watching window $\omega\ (x, y)$, but they change for different local watching window, as done in many dehazing method [17], [26], [31]. Once the initial environmental light and the initial light-scattering attenuation rate are determined, the current local watching window can be initially recovered according to Eq. (2), and then the information loss of which can be calculated. If it reach the maximum number of iterations and the information loss is larger than the pre-set threshold N_{th}, the environmental light and light-scattering attenuation rate should be adjusted iteratively. Then, we traverse the local watching window across the entire image in a non-overlapping manner, and the global changed environmental light and light-scattering attenuation rate will be subsequently achieved.

Here, the size of the local watching window is a key parameter in our algorithm. If the local watching window size is too small, the light-scattering attenuation rate is underestimated and the restored result contains apparent overexposure due to overcorrection. For a larger local window size, on one hand, the information loss constraint becomes more believable, on the other hand, the assumption that light-scattering attenuation rate is constant in a local watching window becomes less appropriate, because too large local watching window is more likely to contain heterogeneous regions and halos may become stronger, time consume of the algorithm increases rapidly as well.

Local watching window selection was tested over a wide range of patch sizes. Fig. 2 shows low-illumination image restoration results using different local watching window sizes. In Fig. 2(b), the window size is 3×3 and the marked regions appear overexposure. In Figs. 2(c) and (d), the patch sizes are 15×15 and 45×45, respectively, the results seem more natural than those in Fig. 2(b), and result in Fig. 2(c) restore more details than Fig. 2(d) in dark regions as marked. Therefore, we set the local watching widow size at 15×15 in the paper, and this size is also recommended by He *et al.* [17].

The block diagram for the compensation of the environmental light and the light-scattering attenuation rate adjustment is shown in Fig. 3. The detailed processes are as follows:

Step 1. Determination of the maximum number of the iteration, denoted as $Iterations$, which is determined by the initial

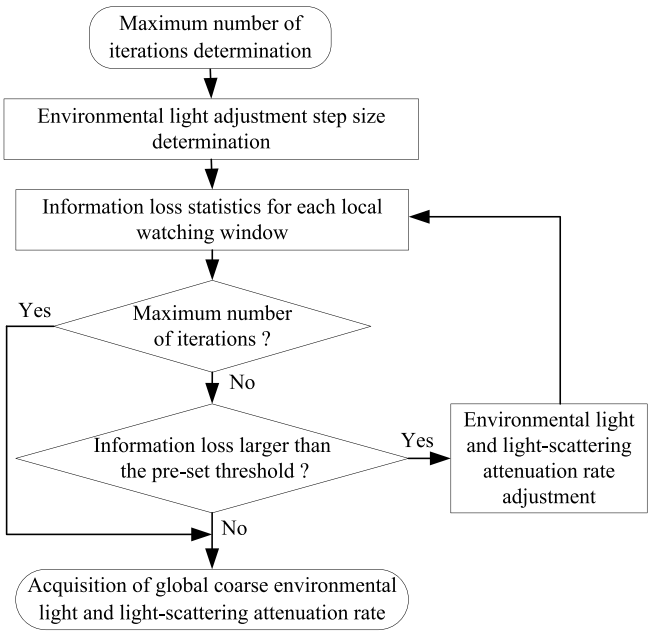

Fig. 3. block diagram for the environmental light and the light-scattering attenuation rate adjustment.

light-scattering attenuation rate t_{ini} and the light-scattering attenuation adjustment step δ. The initial light-scattering attenuation rate equals to the minimum light-scattering attenuation rate in our algorithm, i.e., $t_{ini} = t_{\min}$.

He *et al.* [17] discussed that a typical value of $t_{\min}$ is 0.1 for haze removal, and we found the same situation in our algorithm. Since a smaller $t_{\min}$ tends to over-enhancement in extremely dark regions for low-illumination images and induce pseudo color, amplify noise as well. On the contrast, a larger $t_{\min}$ will bring out under-enhancement for the low-illumination images. Thus, referring to some literatures, we experimentally set $t_{ini} = t_{\min} = 0.1$ in our algorithm to make a trade off. The adjustment step δ for the light-scattering attenuation rate is empirically set to 0.05. The valid range of the light-scattering attenuation rate is [0, 1], thus, the maximum number of iterations can be inferred as $Iterations = (1 - t_{ini})/\delta$.

Step 2. Determination of step size L_{step} for environmental light compensation. The valid display range of the image is [0, 255] for a 8-bit bitmap image, whereas the moderate human visual acceptable pixel intensity is 128. Thus, L_{step} can be formulated as:

$$L_{step} = (128 - L_{ini})/Iterations, \tag{6}$$

where L_{ini} is the initial environmental light for current local watching window.

step 3. Information loss statistics. According to Eq. (2), the initial restored result for the current local watching window, denoted as $\hat{R}_\omega(x, y)$, can be achieved with the initial environmental light L_{ini} and the initial light-scattering attenuation rate. Then, the pixels that are outside the range [0, 255] of $\hat{R}_\omega(x, y)$ in RGB (red, green and blue) three color channels are counted, in which the pixel values that exceed 255 comprise the overflow loss and are denoted as the $upflow$. Conversely, the pixel values of less than 0 comprise the underflow loss and are denoted as the $underflow$. Thus, the total information loss N_{loss} for the current watching window $\omega\ (x, y)$ can be expressed as $N_{loss} = upflow + underflow$.

Step 4. Light-scattering attenuation rate and environmental light adjustment. If the maximum number of iterations not reached and information loss N_{loss} is greater than the preset threshold N_{th}, the light-scattering attenuation rate should be increased by δ, i.e., $t_{ini} = t_{ini} + \delta$. The environmental light is adjusted with step L_{step}; if $upflow > underflow$, L_{ini} should be increased by L_{step}, i.e., $L_{ini} = L_{ini} + L_{step}$. Otherwise, L_{ini} should be decreased by L_{step}, i.e., $L_{ini} = L_{ini} - L_{step}$.

The preset information loss threshold N_{th} is one of the two termination conditions for the environmental light and light-scattering attenuation rate adjustment, i.e., the iteration will terminate if the information loss in a local watching window is smaller than N_{th}. In our algorithm, we set $Nth = 5\% \times size(\omega)$, where $size(\omega)$ is the size of the local watching window $\omega(x, y)$, for the reason that we experimentally found that 5% is belong to the visual unperceivable range, otherwise, a too large N_{th} tends to obvious information loss for the restored low-illumination images and exhibits overexposure or black holes.

Step 5. Acquisition of global coarse parameters. We repeat step 3 and step 4 with the updated light-scattering attenuation rate and environmental light, until the maximum number of iterations is reached or $N_{loss} < N_{th}$. The light-scattering attenuation rate and environmental light for the current window can be achieved. Next, we traverse the local watching window across the entire image in a non-overlapping manner, and the coarse global environmental light and coarse light-scattering attenuation rate are denoted as $\hat{L}_{ini}(x, y)$ and $\hat{t}_{ini}(x, y)$, respectively.

C. Refinement of the Environmental Light and Light-Scattering Attenuation Rate

The previously mentioned environmental light and light-scattering attenuation rate are achieved under the premise that the scene light and scene depth are locally smooth, but it is not in the sense of actual scenes; thus, the sharp edges and these regions produce serious halo effects and block artifacts. Thus, we need a refinement process to suppress the situation. The commonly employed methods include some edge-preserving filters, such as bilateral filters [32] and guide filters [33]. However, the bilateral filter is limited to the elimination of block artifacts, which accounts for effectiveness and efficiency. We adopt the weighted guide filter method [23] for the refinement, and the refined environmental light and light-scattering attenuation rate are denoted as $t(x, y)$ and $L(x, y)$, respectively. The comparison result before and after refinement is show in Fig. 4, which indicates that the halo effects and block artifacts are efficiently eliminated after the refinement.

D. Low-Illumination Image Restoration

The low-illumination image can be directly recovered by solving (2) with the refined parameters $t(x, y)$ and $L(x, y)$. To retain acceptable color rendition, we convert the original image into the HSV (hue, saturation, value) color space, then

Fig. 4. Comparison results before and after a weighted guide filter. (a) the original low-illumination image; (b) the enhanced result without weighted guide filtering; (c) the enhanced result with weighted guide filtering; (d) the final refined light-scattering attenuation rate.

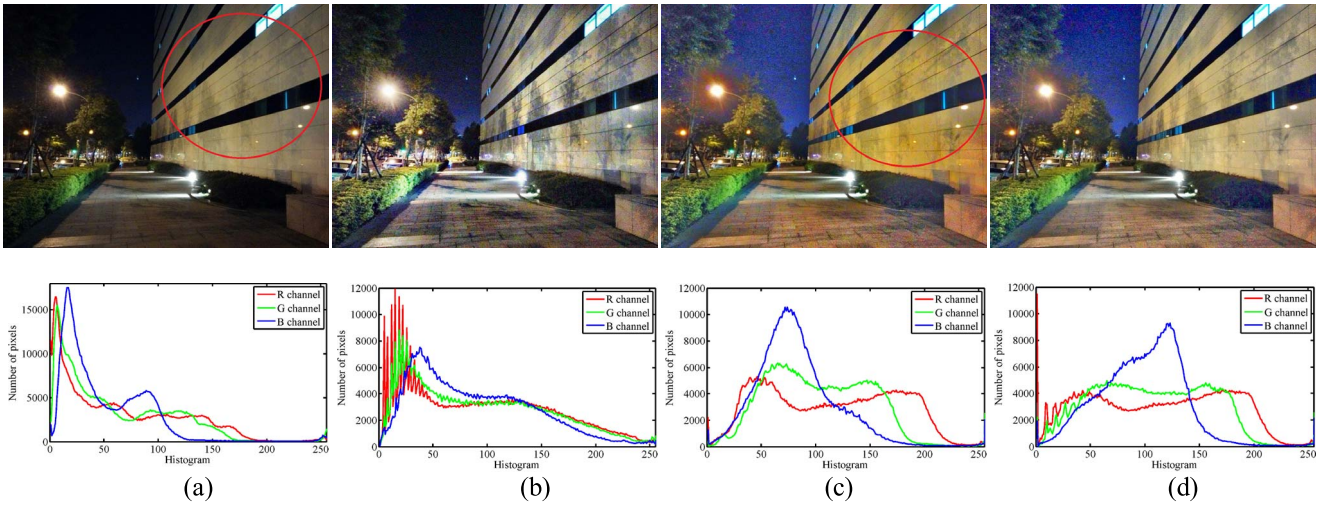

Fig. 5. Color consistency comparison for low-illumination image enhancement. (a) original image and the RGB histogram; (b) enhancement result achieved by contrast limited adaptive HE [5] and the RGB histogram; (c) result achieved by the proposed method in the RGB color space and the RGB histogram; (d) result achieved by the proposed method in HSV color space and the RGB histogram.

we enhance the intensity channel individually and do not change the other two channels.

HSV color model is used to process low-illumination color image in the paper because it has a significant advantage: V component has nothing to do with the image color information and the processed image can keep the original image chroma. In fact, the image corresponding to V component is grayscale image that we are very familiar.

To convert from HSV to RGB, given an HSV color with hue $H \in [0°, 360°]$, saturation $S_{HSV} \in [0, 1]$, and value $V \in [0, 1]$, we obtain the chroma $C = V \times S_{HSV}$.

We can find a point (R1, G1, B1) along the bottom three faces of the RGB cube that has the same hue and chroma as our color (using the intermediate value X for the second largest component of this color): $H' = \frac{H}{60°}$

$$X = C \times \left(1 - \left|H' \bmod 2 - 1\right|\right), \tag{7}$$

$$(R_1, G_1, B_1) = \begin{cases} (0,0,0) & \text{if } H \text{ is undefined} \\ (C,X,0) & \text{if } 0 \le H' \le 1 \\ (0,C,X) & \text{if } 1 \le H' \le 2 \\ (0,X,C) & \text{if } 2 \le H' \le 3 \\ (X,C,0) & \text{if } 3 \le H' \le 4 \\ (X,0,C) & \text{if } 4 \le H' \le 5 \\ (C,0,X) & \text{if } 5 \le H' \le 6, \end{cases} \tag{8}$$

Overlap (when H' is an integer) occurs because the two methods for calculating the value are equivalent: $X = 0$ or $X = C$. We can obtain R, G and B by adding the same amount to each component, to match the value $X = C$.

$$(R, G, B) = (R_1 + m, G_1 + m, B_1 + m), \tag{9}$$

Fig. 5 shows a restored color consistency comparison result for a low-illumination image. Fig. 5(b) is the result achieved by contrast limited adaptive HE [5], Figs. 5(c) and (d) are results achieved by the proposed method in RGB color space and HSV color space, respectively. It is easy to see that the result in Fig. 5(d) appears more natural than those in Figs. 5(b) and (c), especially in the marked regions, which reveal that the result obtained by the proposed method in HSV color space retains significantly better color consistency with the original image.

IV. Results and Discussion

To evaluate the proposed algorithm, extensive tests have been performed using a set of low-illumination images of different scenes, including indoor, outdoor and night vision. Qualitative and quantitative evaluations are explored to comprehensively compare the proposed method with other six new methods, including the ESIHE of Singh and Kapoor [4]; the local content-based bilateral method of Schettini *et al.* [14], which is denoted BFLCC; the multiple-scale Retinex-based method with color restoration of Petro *et al.* [10], denoted MSRCP; the NPEA [22]; the LMCV [19]; and the NHRIC [21].

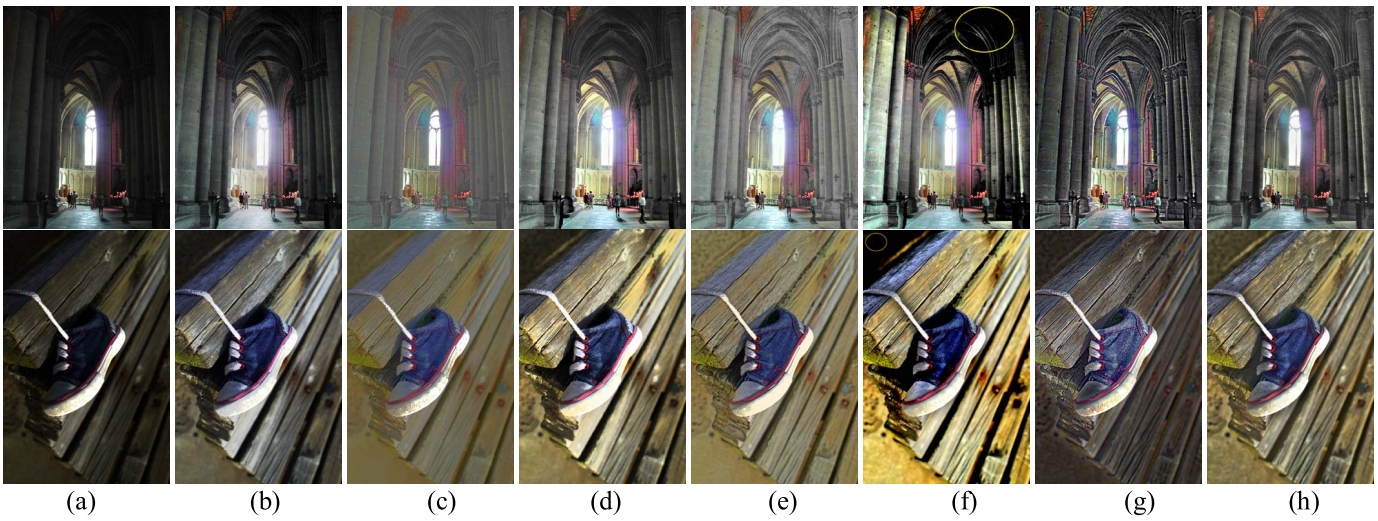

Fig. 6. Comparison results for indoor low-illumination images, from top to bottom are "Cathedral" and "Shoes". (a) the input low-illumination image. (b) ESIHE results. (c) BFLCC results. (d) MSRCP results. (e) NPEA results. (f) LMCV results. (g) NHRIC results. (h) the proposed results.

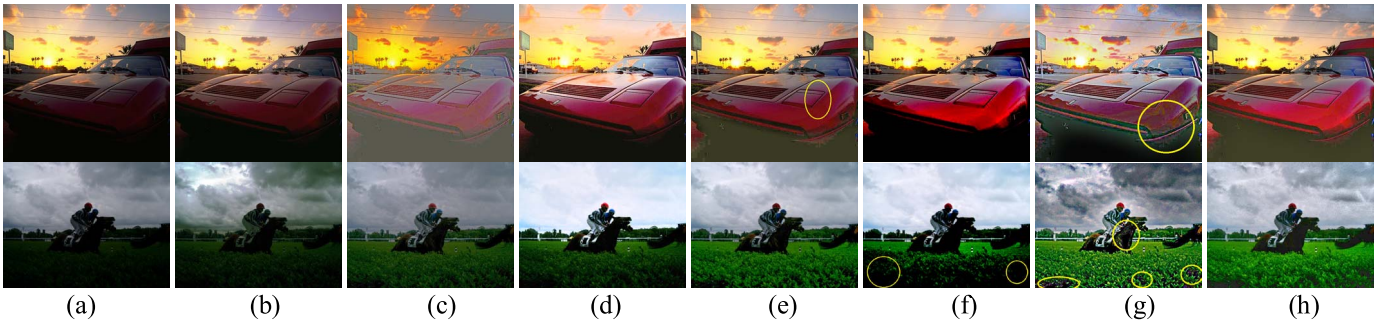

Fig. 7. Comparison results for the cloudy low-illumination images, from top to bottom are "Ferrari" and "Horse". (a) the input low-illumination image. (b) ESIHE results. (c) BFLCC results. (d) MSRCP results. (e) NPEA results. (f) LMCV results. (g) NHRIC results. (h) the proposed results.

A. Qualitative Evaluation

Figs. 6(b) to 9(b) show the results that were enhanced by ESIHE; the contrast of the low-illumination images can be improved. However, the brightness of the bright areas diffuses seriously, as shown in Fig. 8(b). The light in the bright lamp regions in the "People" image diffused significantly. The same situation is observed in the "Cars" image, where the enhanced license plate region is too bright to recognize.

Figs. 6(c) to 9(c) show the results achieved by BFLCC; the method is derived from the Gamma correction, and the correction coefficient is decided by the intensity of the local content. Thus, it can present both dark regions and bright regions. However, the restored color lacks vividness, and the contrast improvement is limited; especially in extremely dark regions. The color is significantly shifted and a vast amount of forged information is induced due to overcorrection.

Figs. 6(d) to 9(d) include the results achieved by MSRCP; to preserve the original colors, MSRCP is applied to the intensity image as discussed by Petro *et al.* [10]. As reflected by the experiment results, the MSRCP method can adequately preserve the original colors and restore a preferable brightness in moderately dark regions; however, it cannot restore rich detail in extremely dark regions.

Figs. 6(e) to 9(e) are results obtained through NPEA. As can be seen that NPEA preserves naturalness, but tiny details are lost, such as the marked regions in the 'Ferrari' image in Fig. 7(e), which highlights the details in the regions of low intensity and produces pseudo details, as shown in Fig. 9(e).

Figs. 6(f) to 9(f) show the results achieved by LMCV; this method can correct the brightness for slightly dark regions, but the information in the dark regions is completely lost, as shown in the marked regions.

Figs. 6(g) to 9(g) include the results produced by NHRIC, as can be seen that this method can restore the sharpness details in bright regions but excessive pseudo color is induced in the dark regions, and the enhanced images lose their original ambience color, as shown in the marked regions.

Figs. 6(h) to 8(h) show the results achieved by the proposed method, which indicate that our method can efficiently improve the contrast, restrain the halo diffusion in bright regions and preserve rich details. Our method can improve the illumination in the dark regions and present rich details. The restored images preserve better color consistency from the input images, and the color is natural.

B. Quantitative Evaluation

Based on these results, we performed a quantitative evaluation using the blind measure of Hautière *et al.* [34]. This quality assessment approach involves computing the ratio of the gradients of the image before and after restoration.

Fig. 8. Comparison results for the night low-illumination images, from top to bottom are "Peoples" and "Cars". (a) the input low light image. (b) ESIHE results. (c) BFLCC results. (d) MSRCP results. (e) NPEA results. (f) LMCV results. (g) NHRIC results. (h) the proposed results.

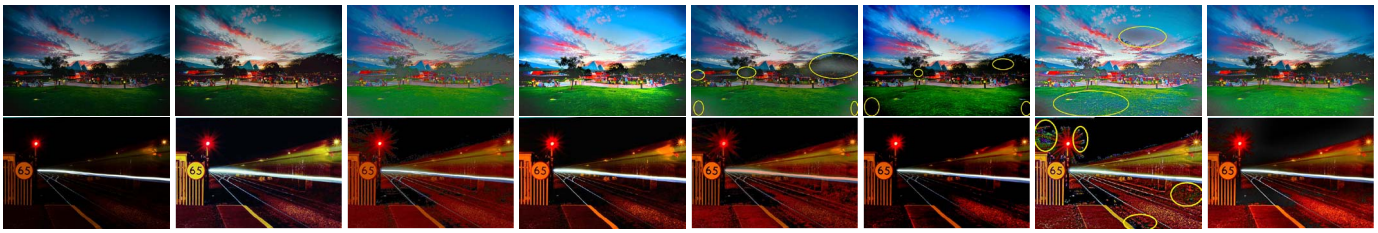

Fig. 9. Comparison results for the daybreak and night low-illumination images, from top to bottom are "Lawn" and "Rail". (a) the input low-illumination image. (b) ESIHE results. (c) BFLCC results. (d) MSRCP results. (e) NPEA results. (f) LMCV results. (g) NHRIC results. (h) the proposed results.

TABLE I

PERCENTAGE OF PIXELS THAT BECOME COMPLETELY BLACK OR COMPLETELY WHITE AFTER RESTORATION ($\sum$)

methods \ images	Cathedral	shoes	Ferrari	Horse	Peoples	Cars	Lawn	Rail	Average
ESIHE	0.17	0.41	**0.00**	0.16	0.06	**0.00**	**0.00**	**0.07**	**0.11**
BFLCC	0.25	0.64	0.01	4.57	0.06	6.03	0.00	27.06	4.83
MSRCP	1.44	0.26	1.01	1.03	0.49	0.91	1.02	1.25	0.93
NPEA	**0.00**	**0.04**	0.02	4.57	**0.00**	6.03	**0.00**	27.11	4.72
LMCV	18.48	14.63	29.23	28.24	6.30	61.67	5.97	53.94	27.31
NHRIC	1.30	0.51	0.26	4.90	0.42	6.34	0.06	27.77	5.20
Proposed	0.13	0.84	0.01	**0.00**	0.26	0.53	**0.00**	3.63	0.68

TABLE II

EDGES THAT ARE NEWLY VISIBLE AFTER RESTORATION (e)

methods \ images	Cathedral	shoes	Ferrari	Horse	Peoples	Cars	Lawn	Rail	Average
ESIHE	0.17	0.24	0.15	0.04	0.35	**0.38**	0.14	0.31	0.22
BFLCC	-0.39	-0.42	-0.15	0.16	-0.69	0.21	-0.03	**0.37**	-0.12
MSRCP	0.03	-0.68	-0.10	0.06	-0.49	0.10	-0.05	0.25	-0.11
NPEA	0.00	0.04	0.07	0.01	0.08	0.22	0.07	0.27	0.10
LMCV	-0.62	0.13	-0.11	-0.32	0.17	-0.27	-0.01	-0.15	-0.15
NHRIC	**0.32**	**0.98**	**0.32**	**0.63**	**0.44**	0.24	**0.17**	0.34	**0.43**
Proposed	0.27	0.32	0.04	0.06	-0.02	0.30	-0.03	0.29	0.15

This approach is based on the concept of the visibility level, which is commonly employed in lighting engineering. In Tables 1 to 3, we considered the eight previously mentioned images (named Cathedral, Shoes, Ferrari, Horse, People, Cars, Lawn and Rail). Table 1 presents the percentage of pixels that become completely black or completely white after restoration, as represented by indicator $\sum$; Table 2 presents the edges that are newly visible after restoration, as represented by the indicator$e$; and Table 3 presents the mean ratio of the gradients at the visible edges, as represented by indicator $\bar{r}$. Theoretically, higher rates produced by e and $\bar{r}$ metrics indicate superior restoration results.

TABLE III
MEAN RATIO OF THE GRADIENTS AT THE VISIBLE EDGES ($\bar{r}$)

methods \ images	Cathedral	shoes	Ferrari	Horse	People	Cars	Lawn	Rail	Average
ESIHE	2.23	2.20	1.30	1.46	2.26	7.96	1.49	3.58	2.81
BFLCC	1.52	2.60	1.70	3.74	1.16	13.97	1.44	4.11	3.78
MSRCP	2.82	**7.92**	2.33	2.99	**4.69**	2.43	2.43	2.74	3.54
NPEA	3.77	3.74	2.00	4.95	3.52	12.78	1.84	4.15	4.59
LMCV	**5.76**	4.44	1.67	3.17	3.47	3.58	2.31	2.33	3.34
NHRIC	5.02	3.84	**3.27**	**8.01**	4.47	**20.12**	**3.41**	**8.95**	**7.14**
Proposed	3.47	3.35	2.01	4.70	2.62	7.44	1.76	3.77	3.64

In contrast, higher rates produced by the $\sum$ metric indicate inferior restoration.

Analyzing the results of Table I, the methods of BFLCC, NPEA, LMCV, and NHRIC yield larger values of $\sum$; however, the situation is substantially better in the ESIHE method and the proposed method. The indicator $\sum$ of the proposed method is kept close to the best values produced by the ESIHE method. But one can observe that the ESIHE method restored limited dynamic range, and the proposed method can reproduce much better color and details in both dark and bright regions.

With regard to the indicator e in Table II, the methods of BFLCC, MSRCP, and LMCV yield negative e because they do not consider information loss during restoration. Only the techniques of ESIHE, NHRIC and the proposed method, are characterized by positive values of the indicator e for the considered images. The NHRIC method increases too strongly the local contrast and as a result it achieves the highest values of indicator e, but the results exhibit serious color shift problems, look unnatural and results in serious noise with false edges in the restored image. However, our method yields moderate indicator e and achieves much more natural results with vivid color.

Moreover, regarding indicator $\bar{r}$ as shown in Table III, the NHRIC method also achieves the highest $\bar{r}$. One can observe from the results that the NHRIC over enhances the local regions of low intensity and produces pseudo details. As a result, false edges are misjudged as visible edges, whereupon inaccurately high restoration rates are produced. Analyzing images of the considered results, one can observe that our method can restore the global illumination with limited information loss and less spurious edges and artifacts.

To the best of our knowledge, the blind measure of Hautière *et al.* [34] is one the most used methods to give a quantitative interpretation for an image restoration operation. However, the indicators of this measure can only partially reveal the level of restoration and degradation. For a more objective evaluation, additional characteristics must be considered; for example, the restored color and the restored naturalness. This task will be one of our future research goals.

V. CONCLUSION

Considering the non-uniform environmental light, we presented a physical lighting model to depict the degradation of low-illumination images, in which, the environmental light and light-scattering attenuation rate are point-wise variables. The restored target image can be directly obtained by solving the model when the parameters are reliably estimated. Thus, we first apply the radiation reflection theory based on Retinex to achieve the initial environmental light, and then coarsely estimate the light-scattering attenuation rate and the environmental light with the information loss constraint via iterative adjustment. Next, the weighted guide filter is utilized to refine the two parameters. Various test results indicate that the proposed method can enhance the details in the dark and bright regions while preserving the tones and information. We avoid over-enhancement and restore distinct visible edges, which significantly improves the appearance of low-illumination images.

Although the performance of the proposed method is adequate compared with that of previous methods, a limitation of our algorithm is observed for images that it produces pseudo color in extremely dark regions.

REFERENCES

[1] R. Hummel, "Image enhancement by histogram transformation," *Comput. Graph. Image Process.*, vol. 6, no. 2, pp. 184–195, 1977.
[2] Y.-T. Kim, "Contrast enhancement using brightness preserving bi-histogram equalization," *IEEE Trans. Consum. Electron.*, vol. 43, no. 1, pp. 1–8, Feb. 1997.
[3] K. Zuiderveld, "Contrast limited adaptive histogram equalization," in *Graphics Gems IV*. San Diego, CA, USA: Academic, 1994, pp. 474–485.
[4] K. Singh and R. Kapoor, "Image enhancement via median-mean based sub-image-clipped histogram equalization," *Optik-Int. J. Light Electron Opt.*, vol. 125, no. 17, pp. 4646–4651, Sep. 2014.
[5] T. Arici, S. Dikbas, and Y. Altunbasak, "A histogram modification framework and its application for image contrast enhancement," *IEEE Trans. Image Process.*, vol. 18, no. 9, pp. 1921–1935, Sep. 2009.
[6] C. Jung and T. Sun, "Optimized perceptual tone mapping for contrast enhancement of images," *IEEE Trans. Circuits Syst. Video Technol.*, vol. 27, no. 6, pp. 1161–1170, Jun. 2017.
[7] E. H. Land, "An alternative technique for the computation of the designator in the retinex theory of color vision," *Proc. Nat. Acad. Sci. USA*, vol. 83, no. 10, pp. 3078–3080, 1986.
[8] D. J. Jobson, Z.-U. Rahman, and G. A. Woodell, "A multiscale retinex for bridging the gap between color images and the human observation of scenes," *IEEE Trans. Image Process.*, vol. 6, no. 7, pp. 965–976, Jul. 1997.
[9] B. Jiang, G. A. Woodell, and D. J. Jobson, "Novel multi-scale retinex with color restoration on graphics processing unit," *J. Real-Time Image Process.*, vol. 10, no. 2, pp. 239–253, 2015.
[10] A. B. Petro, C. Sbert, and J.-M. Morel, "Multiscale retinex," *Image Process. Line*, vol. 4, pp. 71–88, Apr. 2014.

[11] S.-W. Lee, V. Maik, J. Jang, J. Shin, and J. Paik, "Noise-adaptive spatio-temporal filter for real-time noise removal in low light level images," *IEEE Trans. Consum. Electron.*, vol. 51, no. 2, pp. 648–653, May 2005.
[12] Q. Xu, H. Jiang, R. Scopigno, and M. Sbert, "A novel approach for enhancing very dark image sequences," *Signal Process.*, vol. 103, pp. 309–330, Oct. 2014.
[13] M. Kim, D. Park, D. K. Han, and H. Ko, "A novel approach for denoising and enhancement of extremely low-light video," *IEEE Trans. Consum. Electron.*, vol. 61, no. 1, pp. 72–80, Feb. 2015.
[14] R. Schettini, F. Gasparini, S. Corchs, F. Marini, A. Capra, and A. Castorina, "Contrast image correction method," *J. Electron. Imag.*, vol. 19, no. 2, pp. 023005-1–023005-11, 2010.
[15] X. Dong *et al.*, "Fast efficient algorithm for enhancement of low lighting video," in *Proc. IEEE Conf. Multimedia Expo*, Jul. 2011, pp. 1–6.
[16] X. Zhang, P. Shen, L. Luo, L. Zhang, and J. Song, "Enhancement and noise reduction of very low light level images," in *Proc. 21st Int. Conf. Pattern Recognit.*, Nov. 2012, pp. 2034–2037.
[17] K. He, J. Sun, and X. Tang, "Single image haze removal using dark channel prior," *IEEE Trans. Pattern Anal. Mach. Intell.*, vol. 33, no. 12, pp. 2341–2353, Dec. 2011.
[18] C. Liu, H. Zheng, D. Yu, and X. Xu, "A novel method of adaptive traffic image enhancement for complex environments," *J. Sensors*, vol. 2015, pp. 1–9, 2015.
[19] X. Dong and J. Wen, "Low lighting image enhancement using local maximum color value prior," *Frontiers Comput. Sci.*, vol. 10, no. 1, pp. 147–156, 2016.
[20] H. Koschmieder, "Theorie der horizontalen sichtweite: Kontrast und Sichtweite," in *Beiträge Zur Physik Der Freien Atmosphäre*, vol. 12. Munich, Germany: Keim & Nemnich, 1924, pp. 171–181.
[21] J. Zhang, Y. Cao, and Z. Wang. (2016). "Nighttime haze removal with illumination correction." [Online]. Available: https://arxiv.org/abs/1606.01460
[22] S. Wang, J. Zheng, H.-M. Hu, and B. Li, "Naturalness preserved enhancement algorithm for non-uniform illumination images," *IEEE Trans. Image Process.*, vol. 22, no. 9, pp. 3538–3548, Sep. 2013.
[23] Z. Li, J. Zheng, Z. Zhu, W. Yao, and S. Wu, "Weighted guided image filtering," *IEEE Trans. Image Process.*, vol. 24, no. 1, pp. 120–129, Jan. 2015.
[24] E. J. McCartney, *Optics of the Atmosphere: Scattering by Molecules and Particles*. New York, NY, USA: Wiley, 1976.
[25] R. T. Tan, "Visibility in bad weather from a single image," in *Proc. IEEE Conf. Comput. Vis. Pattern Recognit.*, Jun. 2008, pp. 1–8.
[26] R. Fattal, "Dehazing using color-lines," *ACM Trans. Graph.*, vol. 34, no. 1, 2014, Art. no. 13.
[27] C. O. Ancuti and C. Ancuti, "Single image dehazing by multi-scale fusion," *IEEE Trans. Image Process.*, vol. 22, no. 8, pp. 3271–3282, Aug. 2013.
[28] A. J. Preetham, P. Shirley, and B. Smits, "A practical analytic model for daylight," in *Proc. Conf. Comput. Graph. Interact. Techn.*, 1999, pp. 91–100.
[29] D. J. Jobson, Z.-U. Rahman, and G. A. Woodell, "Properties and performance of a center/surround retinex," *IEEE Trans. Image Process.*, vol. 6, no. 3, pp. 451–462, Mar. 1997.
[30] J.-H. Kim, W.-D. Jang, J.-Y. Sim, and C.-S. Kim, "Optimized contrast enhancement for real-time image and video dehazing," *J. Vis. Commun. Image Represent.*, vol. 24, no. 3, pp. 410–425, Apr. 2013.
[31] J.-P. Tarel, N. Hautière, A. Cord, D. Gruyer, and H. Halmaoui, "Improved visibility of road scene images under heterogeneous fog," in *Proc. IEEE Conf. Vehicles Symp.*, Jun. 2010, pp. 478–485.
[32] S. Ghosh and K. N. Chaudhury, "On fast bilateral filtering using Fourier kernels," *IEEE Signal Process. Lett.*, vol. 23, no. 5, pp. 570–573, May 2016.
[33] K. He, J. Sun, and X. Tang, "Guided image filtering," in *Proc. Conf. Eur. Conf. Comput. Vis.*, Sep. 2010, pp. 1–14.
[34] N. Hautière, J.-P. Tarel, D. Aubert, and É. Dumont, "Blind contrast restoration assessment by gradient ratioing at visible edges," *Image Anal. Stereol.*, vol. 27, no. 2, pp. 87–95, 2008.

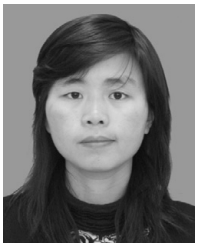

Shun-Yuan Yu received the M.S. degree in materials science and engineering from Xi'an Jiaotong University, Xi'an, China, in 2008. She is currently pursuing the Ph.D. degree with the Faculty of Automation and Information Engineering, Xi'an University of Technology, Xi'an. Her current research interests include digital image processing, video coding, in particular, moving object detection, contrast enhancement, and haze removal.

Hong Zhu received the B.S. degree from Xiamen University, Xiamen, China, in 1984, the M.S. degree from Xi'an University of Technology, Xi'an, China, in 1991, and the Ph.D. degree from University of Fukui, Fukui, Japan, in 1999.

She is currently a Professor and a Doctoral Supervisor with Xi'an University of Technology. Her main research interests include digital image processing, intelligent video surveillance, and pattern recognition.